Acta Crystallographica Section D
Biological Crystallography
ISSN 0907-4449

Structures of cellular retinoic acid binding proteins I and II in complex with synthetic retinoids

Barnali Neel Chaudhuri,[a] Gerard J. Kleywegt,[a] Isabelle Broutin-L'Hermite,[a]† Terese Bergfors,[a] Hans Senn,[b] Peter Le Motte,[b]‡ Olivier Partouche[b] and T. Alwyn Jones[a]*

[a]Department of Cell and Molecular Biology, Uppsala University, Biomedical Center, Box 596, SE-751 24, Uppsala, Sweden, and [b]Department of Pharmaceutical Research, F. Hoffmann–La Roche Ltd, CH-4002 Basel, Switzerland

† Present address: Laboratoire d'Enzymologie et de Biochimie Structurale, Bâtiment 34, CNRS, 1 Avenue de la Terrasse, 91198 Gif-sur-Yvette, France.
‡ Present address: Pharma Research, Pfizer Inc., Department of Molecular Genetics, Groton, CT 06340, USA.

Correspondence e-mail: alwyn@xray.bmc.uu.se

Received 12 March 1999
Accepted 20 August 1999

PDB References: CRABP I–Am80, 2cbr; CRABP II–Ro13-6307, 2cbs; CRABP II–Ro12-7310, 3cbs.

Retinoids play important roles in diverse cellular processes including growth, cell differentiation and vision. Many natural and synthetic retinoids are used as drugs in dermatology and oncology. A large amount of data has been accumulated on the cellular activity of different synthetic retinoids. They are stabilized and transported inside the cell cytoplasm by binding and transport proteins, such as cellular retinol-binding proteins and cellular retinoic acid binding proteins (CRABPs). The structures of human CRABP II in complex with two different synthetic retinoids, Ro13-6307 and Ro12-7310 (at 2.1 and 2.0 Å resolution, respectively) and of bovine CRABP I in complex with a retinobenzoic acid, Am80 (at 2.8 Å resolution) are described. The binding affinities of human CRABP I and II for the retinoids studied here have been determined. All these compounds have comparable binding affinities (nanomolar range) for both CRABPs. Apart from the particular interactions of the carboxylate group of the retinoids with specific protein groups, each structure reveals characteristic interactions. Studying the atomic details of the interaction of retinoids with retinoid-binding proteins facilitates the understanding of the kinetics of retinoid trafficking inside the cytoplasm.

1. Introduction

Retinoids play important roles in a multitude of cellular process including vision, cell differentiation (Saari, 1994; Hofmann & Eichele, 1994), embryonic development and pattern formation (Morriss-Kay & Sokolova, 1996) and programmed cell death (apoptosis; Horn *et al.*, 1996). Both natural and synthetic retinoids possess anticarcinogenic properties (reviewed by Hong & Itri, 1994) and are candidates for drug design (Lotan, 1996). Some of these compounds have been used in the treatment of acute promyelocytic leukemia (Chomienne *et al.*, 1996) and certain skin diseases (Fisher & Voorhees, 1996).

Retinoids exert their effects by binding to nuclear hormone receptors (RAR, RXR) which act as ligand-activated transcription regulators for specific genes (Mangelsdorf *et al.*, 1995; Chambon, 1996). Retinoids are present in the cell in their alcohol, aldehyde, acid and ester forms, which are mutually interconvertible by different enzymes. All-*trans* retinoic acid (RA) and 9-*cis* retinoic acid have been identified as being principally responsible for the interaction with nuclear hormone receptors. Since a shortage or an excess of retinoic acid can cause malfunctioning of retinoid-signalling pathways, maintenance of the retinoid homeostasis in the cell is very important. The concentration of retinoids is controlled in the cell cytoplasm by retinoid-binding proteins, such as cellular

Table 1
IC_{50} values for the binding of various retinoids to human CRABP I and CRABP II.

Ligand	CRABP I IC_{50} (n*M*)	CRABP II IC_{50} (n*M*)
RA	9	25
Ro13-6307	14	6
Ro12-7310	37	58
Am80	140	200
TTNPB	11	12

retinol-binding proteins, cellular retinoic acid binding proteins (CRABPs) and cellular retinaldehyde-binding proteins. Cellular retinoid-binding proteins protect the cell from these amphipathic molecules, protect the retinoids from oxidative degradation and control the availability of retinoids for various metabolic processes (Ross, 1993; Ong *et al.*, 1994; Li & Norris, 1996; Napoli, 1996). The concentration of the retinoid-binding proteins in the cell largely exceeds those of the ligands and they display very high affinity (nanomolar range) for their ligands. These proteins have different spatial and temporal distributions in tissues. It has been shown that the ratio of cellular retinol-binding proteins with and without ligand is crucial for maintaining a balance between the various competitive processes in retinoid metabolism (Napoli, 1996). However, a similar functional role for the CRABPs has yet to be established.

Cellular retinoid-binding proteins from different species display a high degree of sequence similarity and have very similar structures (Banaszak *et al.*, 1994). These proteins belong to a superfamily of lipid-binding proteins which share a β-barrel motif with an internal cavity that binds and stabilizes small hydrophobic/amphipathic ligands (Jones *et al.*, 1988; Banaszak *et al.*, 1994; Newcomer, 1995). Crystal structures of several members, including CRABP I and CRABP II, have been reported (Kleywegt *et al.*, 1994; Thompson *et al.*, 1995; Chen *et al.*, 1998). These structures revealed the nature of the cavity occupied by the retinoids. The orientation of the polar head group of the ligand within the protein groups is determined by a few specific polar interactions in the interior of the cavity. Thus, in spite of the overall structural similarity and sequence homology, retinoid-binding proteins are capable of distinguishing between different retinoids with a high degree of specificity (Ong & MacDonald, 1987; Levin *et al.*, 1988; Giguère *et al.*, 1990; Fiorella *et al.*, 1993). The structural basis of this recognition was proposed by Jones *et al.* (1988).

The strong anticarcinogenic activity of the synthetic retinoids and their varying specificity, toxicity and stability compared with their naturally occurring counterparts make them important in medical research. A considerable amount of data has been accumulated on the binding of these synthetic compounds to various retinoid-binding proteins and nuclear receptors. Many of the synthetic retinoids are reported to have similar or even higher biological activity and lower toxicity than their natural counterparts. An in-depth understanding of the details of their binding to the cellular carrier proteins is therefore of interest for drug design.

Here, we present the crystal structures of human CRABP II in complex with two synthetic retinoids, Ro13-6307 at 2.0 Å and Ro12-7310 at 2.1 Å resolution, and of bovine CRABP I in complex with a synthetic retinobenzoic acid, Am80, at 2.8 Å resolution. Ro13-6307 is an unselective agonist of RAR with potential application in dermatology and oncology (Apfel *et al.*, 1992). Ro12-7310 is an inactive metabolite of etretinate (tigason), a drug for the treatment of psoriasis (Peck & DiGiovanna, 1994). A number of retinobenzoic acids, including Am80, Am580 and TTNPB (Kagechika *et al.*, 1988), have been used in dermatology and oncology. Am80 is a selective agonist of RAR-α and has been tested in clinical trials of cancer patients with advanced acute promyelocytic leukemia (Tobita *et al.*, 1997). These crystal structures provide important information about CRABP–drug interactions.

2. Materials and methods

2.1. Expression, purification and binding studies of CRABP I and II

Expression and purification of recombinant CRABP I and II have been described by Bergfors *et al.* (1994). For the binding studies, purified protein was diluted in the binding buffer (10 m*M* Tris–HCl pH 8.0, 1.5 m*M* EDTA, 2 m*M* DTT, 10% glycerol, 1 m*M* PMSF, 0.8 *M* KCl, 10 µg ml^{-1} aprotinin, 10 µg ml^{-1} leupeptin, 3 mg ml^{-1} γ-globulin) and used in competition binding experiments. Extracts were incubated on ice for 3 h with ^{3}H-labelled all-*trans* retinoic acid (5 n*M*) in the presence or absence of varying concentrations of unlabelled ligand. Complexed protein was separated from ligand-free protein using a NAP-5 desalting column (Pharmacia, Sweden) and the radioactivity was determined by liquid-scintillation counting. IC_{50} values were calculated from competition binding curves from at least three independent experiments (Table 1).

2.2. Crystallization

All crystallization trials were carried out using the hanging-drop vapour-diffusion method (McPherson, 1982).

2.2.1. Preparation of CRABP–retinoid complexes. The CRABP I–Am80 complex was prepared as described by Bergfors *et al.* (1994). Ro12-7310 and Ro13-6307 were solubilized in DMSO and added in molar excess to the concentrated solution of recombinant human CRABP II in the dark. The complex was filtered through a 0.2 µm filter (Anapore, Whatman) prior to crystallization experiments.

2.2.2. CRABP II–Ro13-6307. The crystallization drop contained 2 µl of the protein (24.6 mg ml^{-1}) in 50 m*M* Tris–HCl pH 8.0 and 2 µl of reservoir solution. The reservoir solution contained 20% monomethyl PEG 5000 and 0.1 *M* sodium acetate pH 5.5. Crystals were grown in the dark at room temperature.

2.2.3. CRABP II–Ro12-7310. The crystallization drop contained 2 µl of the protein (25 mg ml^{-1}) in 20 m*M* Tris–HCl pH 8.0 and 2 µl of reservoir solution. The drop was equilibrated against 20% monomethyl PEG 5000, 0.2 *M* Tris–HCl

Table 2
Crystal and data statistics.

Values in parentheses are for the highest resolution shell.

Complex	CRABP II–Ro13-6307	CRABP II–Ro12-7310	CRABP I–Am80
Space group	$P2_12_12_1$	$P2_12_12_1$	$P3_221$
Resolution (Å)	45–2.1 (2.15–2.1)	48–2.0 (2.03–2.0)	38–2.8 (2.95–2.8)
Unit-cell parameters (Å)	45.2, 47.6, 74.8	38.0, 48.3, 83.8	133.5, 133.5, 40.5
Average redundancy	4.3 (4.3)	3.2 (3.0)	3.7 (3.8)
Completeness (%)	97.7 (97.7)	91.9 (93.3)	97.6 (95.7)
$R_{\rm merge}$†	0.061 (0.16)	0.029 (0.11)	0.086 (0.26)
Reflections with $I/\sigma(I) > 3$ (%)	89.0 (79.9)	93.4 (84.0)	84.9 (63.4)
$\langle I/\sigma(I)\rangle$	25.9 (11.6)	35.1 (12.2)	20.2 (5.2)

† $R_{\rm merge} = \sum_h \sum_i |I_{h,i} - \langle I_h\rangle| / \sum_h \sum_i |I_{h,i}|$.

(pH 8.5) and 0.2 *M* LiCl. Crystals were grown in the dark at 277 K.

2.2.4. CRABP I–Am80. The crystallization drop contained 2 µl of the protein (19 mg ml^{-1}) in 50 m*M* Tris–HCl pH 8.0, 0.1% β-octyl glucoside and 1 m*M* β-mercaptoethanol and 2 µl of the reservoir solution. The reservoir contained 30% PEG 4000, 0.2 *M* Li_2SO_4 and 0.1 *M* Tris–HCl (pH 8.0). Crystals were grown at 277 K. Am80 is not light-sensitive and so no light precautions were required.

2.3. Data collection and processing

Data from the CRABP crystals were collected at room temperature or at 277 K on an in-house Rigaku R-AXIS IIC imaging-plate system mounted on a Rigaku rotating-anode generator (λ = 1.54 Å). *DENZO*/*SCALEPACK* (Otwinowski & Minor, 1997) and *SCALA* (Collaborative Computational Project Number 4, 1994) were used for indexing, processing and scaling the data. Details of the data collection, processing and merging are shown in Table 2.

2.4. Structure solution

Crystals of the CRABP II–Ro13-6307 complex were isomorphous to the CRABP II–RA complex (Kleywegt *et al.*, 1994). All other structures were solved by the molecular-replacement method (Rossmann, 1972) as implemented in the program *AMoRe* (Navaza, 1994), using the retinoic acid complex of each protein as a search model (PDB codes: CRABP I, 1cbr; CRABP II, 1cbs). Data in the resolution range 15.0–4.0 Å were used in the molecular-replacement calculations for all structures.

2.4.1. CRABP II–Ro13-6307. Crystals were isomorphous to those of the RA complex of the protein. 50 cycles of rigid-body refinement in *X-PLOR* (Brünger, 1990) using the model of the RA complex without ligand and water molecules were sufficient to obtain a starting model with an *R* factor of 0.33 (15.0–4.0 Å data).

2.4.2. CRABP II–Ro12-7310. The correlation coefficient was 0.80 and the *R* factor was 0.36 for one molecule in the asymmetric unit (15.0–4.0 Å data, space group $P2_12_12_1$).

2.4.3. CRABP I–Am80. This complex had two molecules in the asymmetric unit. The correct space group was found to be $P3_221$, since translation-function solutions for this space group showed much better correlation coefficients than those in the enantiomorphic space group $P3_121$. After rigid-body refinement, the solution had a correlation coefficient of 0.70 with an *R* factor of 0.34 (15.0–4.0 Å data).

2.5. Refinement

All three structures were refined with *X-PLOR* (Brünger, 1990) and *CNS* (Brunger *et al.*, 1998), using high-temperature simulated-annealing protocols (Brünger *et al.*, 1990). Between refinement cycles, models were rebuilt in *O* (Jones *et al.*, 1991). A test set of about 8% of the data was kept aside to monitor the free *R* factor during the course of refinement (Brünger, 1992). Ligand density was clearly visible in all the complexes. Dictionaries for all three ligand molecules were generated using *XPLO2D* (Kleywegt & Jones, 1997). Since coordinates for Ro13-6307 and Am80 were unavailable, standard geometry was imposed during refinement. Coordinates of tigason (H. Senn, unpublished data), an ester derivative of Ro12-7310, were used to build the initial model of Ro12-7310.

2.5.1. CRABP II with Ro13-6307 and Ro12-7310. Both complexes have one molecule in the asymmetric unit. Each ligand was placed in the density based on $2F_o - F_c$ and $F_o - F_c$ maps after the first round of refinement. Water molecules were added in the final stages of the refinement. Grouped *B*-factor refinement was used until the final stage of the refinement, when individual restrained isotropic *B* factors were refined.

2.5.2. CRABP I–Am80. This structure has twofold NCS. The structure was initially refined with NCS restraints, since this gave lower $R_{\rm free}$ values than refinement with NCS constraints. Tighter restraints were used for the main-chain atoms than for the side-chain

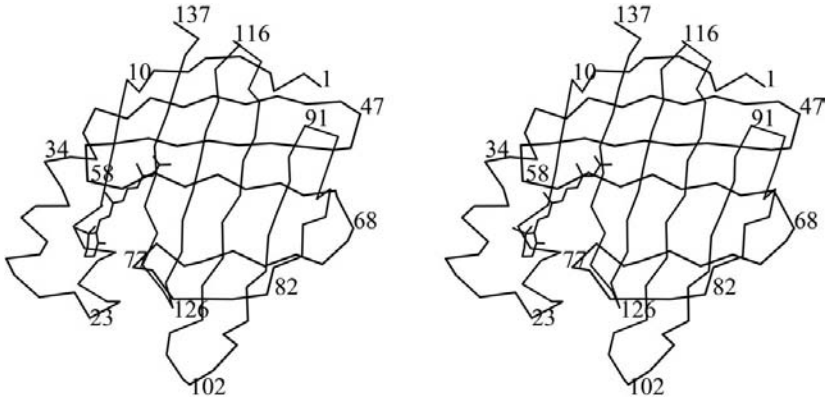

Figure 1
C^α trace of CRABP II in complex with retinoic acid (PDB code 1cbs).

Table 3
Refinement and model statistics.

N/A: not applicable. pm: per molecule.

Complex	CRABP II–Ro13-6307	CRABP II–Ro12-7310	CRABP I–Am80
Resolution range (Å)	10–2.1	10–2.0	30–2.8
No. of reflections	8770	9196	9305
R factor†	0.198	0.199	0.228
R_{free}†	0.230	0.244	0.266
Non-crystallographic symmetry	N/A	N/A	Twofold, constrained
No. of water molecules	52	66	8 pm
Rm.s.d. bond lengths (Å)‡	0.006	0.006	0.008
Rm.s.d. bond angles (°)‡	1.4	1.5	1.4
Average *B*, protein (Å^2)	22.6	23.4	40.0
Average *B*, ligand (Å^2)	17.8	20.2	22.9
Average *B*, water (Å^2)	30.6	30.2	25.8
R.m.s. ΔB bonded atoms (Å^2)	2.1	1.4	N/A
Ramachandran outliers§ (%)	2.4	2.4	1.6
No. of residues with pepflip¶ > 2.5 Å	2	2	3 pm
No. of residues with RSC¶ > 1.5 Å	2	2	1 pm
No. of residues with RSCC†† < 0.7	2	1	0 pm
Overall DACA score‡‡	0.1	0.1	0.0
Overall *G* factor§§	0.33	0.34	0.30

† *R* factor = $\sum ||F_o| - |F_c|| / \sum |F_o|$; R_{free} is the same but calculated for a subset of reflections not used in the refinement; F_o and F_c are the observed and calculated structure factors, respectively. ‡ Calculated with *CNS* (Brünger *et al.*, 1998), using the Engh & Huber (1991) force field. § Calculated with *MOLEMAN2* (G. J. Kleywegt, unpublished program), using the definition of Kleywegt & Jones (1996). ¶ Pepflip and RSC values calculated using *O* (Jones *et al.*, 1991). †† RSCC (real-space correlation coefficient; Jones *et al.*, 1991) values calculated using *CNS* (Brünger *et al.*, 1998). ‡‡ Calculated using *WHATIF* (Vriend & Sander, 1993). §§ Calculated using *PROCHECK* (Laskowski *et al.*, 1993).

atoms. Electron density for Am80 was clearly visible in the $2F_o - F_c$ and $F_o - F_c$ maps and a planar model of Am80 was built into the density. In a test refinement, the ligand model showed slight deviations from planarity if the dihedral angles of the freely rotatable bonds in Am80 were not restrained. However, because of the limited resolution, those dihedral angles were kept restrained in order to enforce planarity (Kleywegt & Jones, 1995). Temperature factors were modelled by group (two *B* factors per residue). A few water molecules were added using the program *PEKPIK* (Collaborative Computational Project, Number 4, 1994) based on $2F_o - F_c$ and $F_o - F_c$ density maps and hydrogen-bonding contacts. Since the two molecules were very similar to each other, NCS constraints were imposed in the final rounds of the refinement. Averaged electron-density maps (calculated using *RAVE*, Kleywegt & Jones, 1994*a*) were used for rebuilding the model.

2.6. Quality of the final models

Details of the refinement and model statistics are listed in Table 3. Ramachandran plots (Ramakrishnan & Ramachandran, 1965) look satisfactory for all three structures with less than 3% outliers, most of which lie close to allowed regions (Kleywegt & Jones, 1996). The only exception is Asp126, but this residue is also an outlier in the CRABP–RA complexes and has good density. All figures (except Fig. 3) were prepared using *O* and *OPLOT* (M. Kjeldgaard, unpublished program). *VOIDOO* (Kleywegt & Jones, 1994*b*) and *ASA* (Lee & Richards, 1971) were used for cavity and accessible surface-area calculations, respectively.

3. Results and discussion

3.1. Overall description

In all three complexes, the protein structures are essentially identical to those reported earlier (Kleywegt *et al.*, 1994; PDB codes 1cbr, 1cbq and 1cbs). The overall structure is composed of a ten-stranded antiparallel β-barrel (strands are numbered βA to βJ) with a helix–turn–helix segment (αI and αII) inserted between βA and βB (Banaszak *et al.*, 1994; Fig. 1). The r.m.s.d. on C^α atoms between each of these three complexes and the RA-bound complex is less than 0.5 Å. If the protein structures are superimposed, the bound retinoids are all coplanar and occupy approximately the same space as RA in CRABP I and II (Figs. 2*a* and 2*b*). The narrow tunnel-like cavity mouth is more hydrophobic and fits snugly around the non-polar part of the amphipathic ligands in all the CRABP complexes (Kleywegt *et al.*, 1994). This shape complementarity is not maintained in the cavity interior, although there is electrostatic complementarity. The carboxylate group is inclined with respect to the isoprenoid plane of the retinoid in all structures. The orientation of the carboxylate group is the same with respect to the Arg-Tyr-Arg triad (Arg111, Tyr134 and Arg132; CRABP II numbering) of the protein in all the synthetic retinoids and in RA, including the conserved water-mediated interaction with Arg111. Both the N^η and N^ε atoms of the guanido group of Arg132 are within hydrogen-bonding distance of the retinoid carboxylate group in all three structures. Most of the residues that line the cavity surface have similar conformations as in the CRABP I and II structures complexed with RA. However, subtle differences exist in each case, owing to the difference in chemical structure of the synthetic retinoids (Fig. 3). Each complex contains a few bound water molecules inside the cavity together with the ligand. The exact location of the water molecules is not necessarily conserved, except for the water molecule which mediates the interaction between the carboxylate group of the ligands and Arg111.

Binding data for RA, Ro13-6307 and Ro12-7310 with CRABP I and II are shown in Table 1. The binding constants are quite similar to each other, except for Am80, whose binding is slightly weaker.

3.2. Human CRABP II complex with Ro13-6307

All the cavity-lining residues in the CRABP II–Ro13-6307 complex are identical in conformation to those in the CRABP II–RA complex, except for Arg59. Ro13-6307 contains an aromatic ring fused to the β-ionone ring (Fig. 3*b*) and Arg59 forms a charge/π-cloud interaction with this aromatic ring (Fig. 4). This residue also forms a hydrogen bond with a main-chain carbonyl O atom (Val76), which helps to anchor its

orientation. This arginine side chain forms a hydrogen bond to the side chain of Gln74 in all other CRABP II structures and a salt bridge to the side chain of Glu74 in CRABP I.

3.3. Human CRABP II in complex with Ro12-7310

In the structures of CRABP I and II bound to RA, the β-ionone moiety of RA is stacked between the N-terminal of the αII helix and the βC–βD turn in the open cavity mouth (Kleywegt *et al.*, 1994). In Ro12-7310, the β-ionone ring of RA is replaced by a planar aromatic ring (Fig. 3*c*). This aromatic ring plane is tilted by $\sim 60^\circ$ out of the isoprenoid plane (torsion angle C5—C6—C7—C8 = -56°), thus mimicking the structure of the β-ionone ring of RA in its complex with CRABPs (Fig. 5). The environment near the cavity mouth is essentially identical to that in the RA-bound form, except that helix αII is slightly shifted compared with the RA and Ro13-6307 complexes (for residues 23–35, the r.m.s.d. on C^α atoms is 0.6 Å between the Ro12-7310 and RA complexes; Fig. 5). The side chain of residue Leu28, in particular, has moved into the cavity in the Ro12-7310 complex, filling up the empty space. This residue buries 45 Å^2 of accessible surface area (calculated using *ASA* with a 1.4 Å probe radius) upon complexation, which is approximately 15 Å^2 more than its buried surface area in the RA and Ro13-6307 complexes. The hydroxyl group attached to the aromatic ring of the ligand lies outside the cavity and interacts with an external water molecule.

3.4. Bovine CRABP I in complex with Am80

Human CRABP I and bovine CRABP I differ by only one residue, Ala80 (human) *versus* Pro80 (bovine), both of which are distant from the binding site. Binding studies have shown a weaker binding affinity for Am80 (Fig. 3*d*) compared with RA for human CRABP I (Table 1) and it is safe to assume that the same is true for the bovine protein. Instead of the long isoprenoid tail of RA, Am80 has two rigid benzene rings joined by a carboxamide link. In the crystal structure, we observed that the two benzene rings of Am80 are *trans* to each other.

The guanidium group of Arg131 (132 in CRABP II) is close to the aromatic ring of the benzoic acid moiety of Am80 and to Phe15, forming a weak charge/π-cloud interaction with both. Arg131, together with Tyr133 (134 in CRABP II) and Arg111 (the Arg-Tyr-Arg triad), makes the usual hydrogen bonds with the carboxylate group of Am80.

A buried water molecule forms hydrogen bonds with the side-chain amino group of Arg59, the carbonyl O atom of

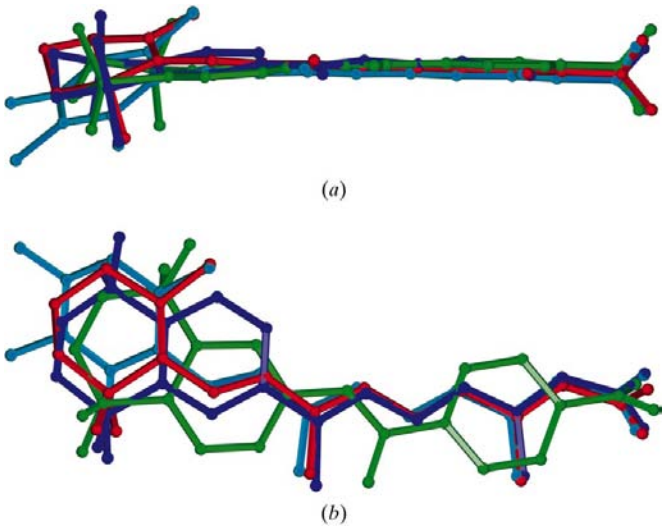

Figure 2
RA (in CRABP I, PDB code 1cbs; red), Am80 (green), Ro13-6307 (blue), Ro12-7310 (sky-blue) in superimposed CRABP structures: (*a*) sideways view (*b*) top view.

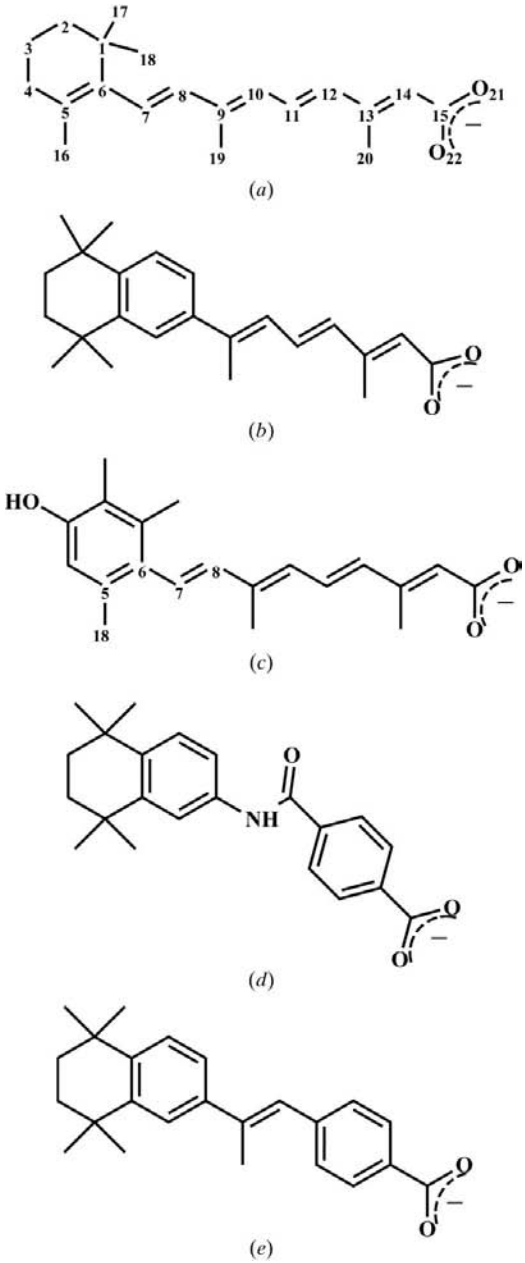

Figure 3
The chemical structures of (*a*) all-*trans* retinoic acid, (*b*) Ro13-6307, (*c*) Ro12-7310, (*d*) Am80 and (*e*) TTNPB.

Val76 and the N atom of the central amide moiety of Am80 (Fig. 6). The carbonyl O atom of the amide moiety of Am80 is 4.0 and 3.5 Å away from the hydroxyl and methyl groups of nearby Thr56, respectively. The hydroxyl group of Thr56 interacts with the carbonyl O atom of Arg59 in both the RA and the Am80 complexes.

4. Conclusions

A structural comparison of the various CRABP complexes reveals the salient features of CRABP–retinoid interactions. All the ligands have conformations which are elongated and similar in shape to RA (Fig. 2). This allows them to fit inside the tunnel-like cavity mouth and to maintain proper electrostatic interactions. The common theme of the retinoid carboxylate group tilted with respect to the isoprenoid plane and interacting with the Arg-Tyr-Arg triad (the so-called P2-myelin motif, Jones *et al.*, 1988) is preserved in all structures. Although the retinoids only fill part of the large cavity, all three ligands lose more than 80% of their water-accessible surface area upon complexation. Most of the cavity-lining residues surrounding the hydrophobic cavity mouth (helix αII, the βC–βD loop and the βE–βF loop) lose accessible surface area on formation of the complexes. Thus, extensive hydrophobic and polar interactions determine the high binding affinity in all the structures. Two isomers of RA, 9-*cis* retinoic acid and 13-*cis* retinoic acid, have very low binding affinity for CRABPs (H. Senn, unpublished data), presumably owing to their kinked conformation.

The orientation of the β-ionone ring with respect to the isoprenoid tail can be described by the dihedral angle C5—C6—C7—C8, which is −33° in the CRABP–RA complexes (Kleywegt *et al.*, 1994; Fig. 3*a*). The equivalent dihedral angle in both Ro13-6307 and Am80 is 180°, because of the restraints imposed by the planar aromatic ring (Figs. 3*b* and 3*d*). In Ro12-7310, the corresponding dihedral angle C5—C6—C7—C8 is −56°. The crystal structure of Ro12-7310 is not known, but that of an ester derivative (tigason) is known (H. Senn, unpublished data) and the corresponding dihedral angle is −100°. The change of 44° in this dihedral angle is probably induced by the surrounding protein residues. It is interesting to note that the binding cavity forces this non-physiological ligand to adopt an RA-like conformation at the expense of a closer contact between C8 and C18 (3.2 Å, compared with 3.7 Å in the crystal structure of tigason).

In the Ro13-6307 complex, instead of forming a hydrogen bond with Gln74 as in the other complexes, the Arg59 side chain forms a charge/π-cloud interaction with the aromatic ring of the retinoid and a hydrogen bond with the carbonyl O atom of Val76 in the βE–βF turn. However, the binding strength of Ro13-6307 is not very different from that of RA (Table 1). Unlike in the Ro13-6307 complex, the guanidium group of the Arg59 side chain in the Am80 complex does not have any interactions with the alkyl-substituted benzene ring of Am80. This arginine side chain forms a salt bridge to Glu74 in both CRABP I–RA and CRABP I–Am80 (Fig. 6). Although both Arg59 and Glu74 have high temperature factors (>40 Å^2), the overall orientation of their side chains is well defined by the density. The strong ion-pair interaction may prevent the Arg59 side chain from reorienting itself. Arg59 is also involved in a water-mediated interaction with the polar groups of Am80. In all these structures, the non-polar side-chain atoms of Arg59 are part of the surface that covers the ligand. In both the Ro13-6307 complex and the Am80 complex, this residue loses ∼50 Å^2 surface area upon complexation, which is at least 10 Å^2 more than in other CRABP I and II complexes. This is probably because of the presence of an aromatic ring fused to the β-ionone ring.

The central feature of the CRABP I–Am80 interaction is the placement of a polar moiety (the carboxamide group) in a largely hydrophobic region of the cavity. One of the two polar groups (the —NH— group) is

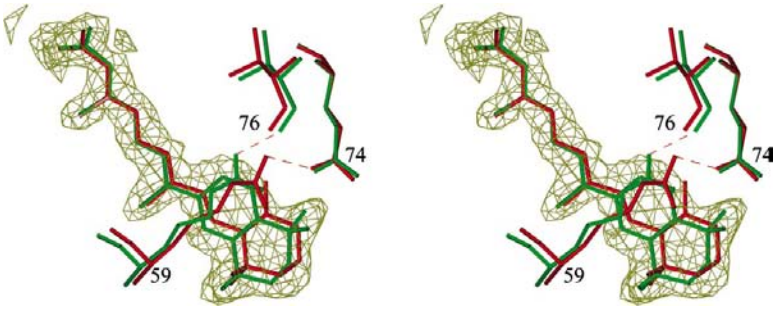

Figure 4
Comparison of the binding of Ro13-6307 to CRABP II (green) with that of RA (Kleywegt *et al.*, 1994; PDB code 1cbs; red). σ_A-weighted simulated-annealing omit density (Read, 1986; Hodel *et al.*, 1992) is shown for the ligand. Hydrogen bonds are indicated by dashed lines.

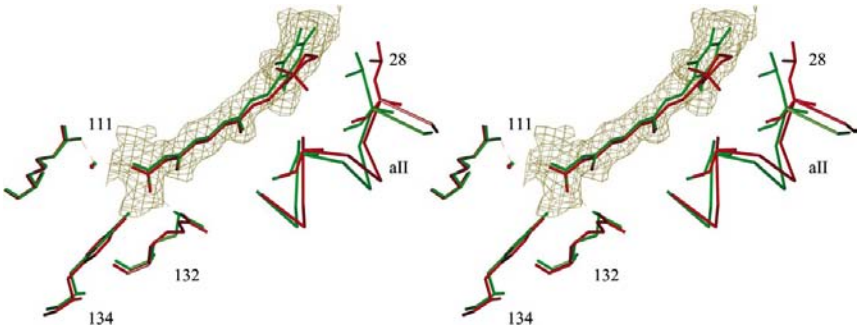

Figure 5
Interactions of Ro12-7310 with the Arg-Tyr-Arg triad and the αII helix (with residue Leu28) of CRABP II, as observed in the crystal structure of CRABP II–Ro12-7310 (green). All-*trans* retinoic acid and the αII helix of the CRABP II–RA complex (Kleywegt *et al.*, 1994; PDB code 1cbs; red) are also shown. σ_A-weighted simulated-annealing omit density for the ligand (Read, 1986; Hodel *et al.*, 1992) is shown. Hydrogen-bonding interactions are indicated by dashed lines.

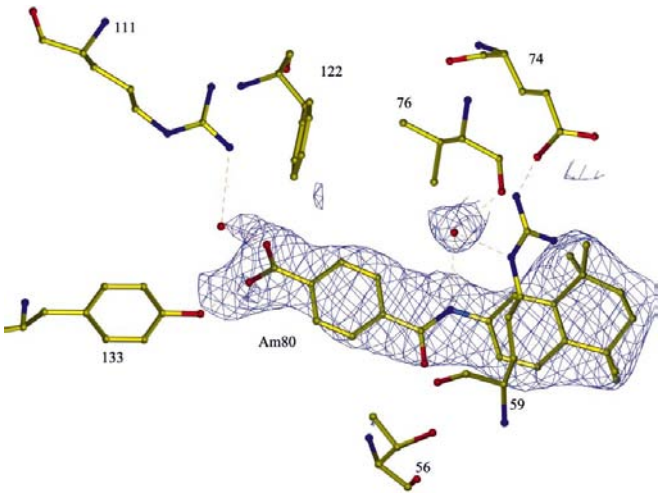

Figure 6
The interaction of Am80 with CRABP I (yellow C atoms; red O atoms; blue N atoms). σ_A-weighted simulated-annealing omit density for the ligand (Read, 1986; Hodel *et al.*, 1992) is shown. Hydrogen-bonding interactions are indicated by dashed lines.

stabilized by water-mediated interactions. The hydrogen-bonding capacity of the carbonyl group is not satisfied. TTNPB, which is identical to Am80 (Fig. 3*e*) except that the central polar group is replaced by a $-C(CH_3)=CH-$ group, forms a stronger complex with CRABPs (Table 1). This indicates that the polar moiety in the region of the cavity surrounded by many hydrophobic residues makes a significant contribution to the weakening of the complexation.

The diverse biological functions of naturally occurring retinoids (RA and 9-*cis* retinoic acid) and concomitant undesired side effects make them less suitable as drugs. Synthetic retinoids with a desired level of specificity can be used to narrow down the range of retinoid activity and associated side effects. Crystal structures of cellular retinoid-binding proteins with and without various synthetic retinoids provide clues about their flexibility in accommodating structurally varied retinoids. This is fundamentally important for low-solubility drug trafficking, which might be useful for new drug design.

This work was supported by the Swedish Natural Science Research Council and Uppsala University. BNC thanks Drs Jinyu Zou, Alex Cameron and Tom Taylor for useful discussions and help.

References

Apfel, C., Bauer, F., Crettaz, M., Forni, L., Kamber, M., Kaufmann, F., LeMotte, P., Pirson, W. & Klaus, M. (1992). *Proc. Natl Acad. Sci. USA*, **89**, 7129–7133.

Banaszak, L., Winter, N., Xu, Z., Bernlohr, D. A., Cowan, S. & Jones, T. A. (1994). *Adv. Protein Chem.* **45**,89–151.

Bergfors, T., Kleywegt, G. J. & Jones, T. A. (1994). *Acta Cryst.* D**50**, 370–374.

Brünger, A. T. (1990). *X-PLOR. A System for Crystallography and NMR.* Yale University, New Haven, Connecticut, USA.

Brünger, A. T. (1992). *Nature (London)*, **355**, 472–475.

Brunger, A. T., Adams, P. D., Clore, G. M., DeLano, W. L., Gros, P., Grosse-Kunstleve, R. W., Jiang, J.-S., Kuszewski, J., Nilges, M., Pannu, N. S., Read, R. J., Rice, L. M., Simonson, T. & Warren, G. L. (1998). *Acta Cryst.* D**54**, 905–921.

Brünger, A. T., Krukowski, A. & Erickson, J. W. (1990). *Acta Cryst.* A**46**, 585–593.

Chambon, P. (1996). *FASEB J.* **10**, 940–954.

Chen, X., Tordova, M., Gilliland, G. L., Wang, L., Li, Y., Yan, H. & Ji, X. (1998). *J. Mol. Biol.* **278**, 641–653.

Chomienne, C., Fenaux, P. & Degos, L. (1996). *FASEB J.* **10**, 1025–1030.

Collaborative Computational Project, Number 4 (1994). *Acta Cryst.* D**50**, 760–763.

Engh, R. A. & Huber, R. (1991). *Acta Cryst.* A**47**, 392–400.

Fiorella, P. D., Giguère, V. & Napoli, J. L. (1993). *J. Biol. Chem.* **268**, 21545–21552.

Fisher, G. J. & Voorhees, J. J. (1996). *FASEB J.* **10**, 1002–1013.

Giguère, V., Lyn, S., Yip, P., Siu, C. H. & Amin, S. (1990). *Proc. Natl Acad. Sci. USA*, **87**, 6233–6237.

Hodel, A., Kim, S.-H. & Brünger, A. T. (1992). *Acta Cryst.* A**48**, 851–858.

Hofmann, C. & Eichele, G. (1994). *The Retinoids: Biology, Chemistry and Medicine*, edited by M. B. Sporn, A. B. Roberts & D. S. Goodman, pp. 387–441. New York: Raven Press.

Hong, W. K. & Itri, L. M. (1994). *The Retinoids: Biology, Chemistry and Medicine*, edited by M. B. Sporn, A. B. Roberts & D. S. Goodman, pp. 597–630. New York: Raven Press.

Horn, V., Minucci, S., Ogryzko, V. V., Adamson, E. D., Howard, B. H., Levin, A. A. & Ozato, K. (1996). *FASEB J.* **10**, 1071–1077.

Jones, T. A., Bergfors, T., Sedzik, J. & Unge, T. (1988). *EMBO J.* **7**, 1597–1604.

Jones, T. A., Zou, J. Y., Cowan, S. W. & Kjeldgaard, M. (1991). *Acta Cryst.* A**47**, 110–119.

Kagechika, H., Kawachi, E., Hashimoto, Y., Himi, T. & Shudo, K. (1988). *J. Med. Chem.* **11**, 2182–2192.

Kleywegt, G. J., Bergfors, T., Senn, H., Le Motte, P., Gsell, B., Shudo, K. & Jones, T. A. (1994). *Structure*, **2**, 1241–1258.

Kleywegt, G. J. & Jones, T. A. (1994*a*). *Proceedings of the CCP4 Study Weekend. From First Map to Final Model*, edited by S. Bailey, R. Hubbard & D. Waller, pp. 59–66. Warrington: Daresbury Laboratory.

Kleywegt, G. J. & Jones, T. A. (1994*b*). *Acta Cryst.* D**50**, 178–185.

Kleywegt, G. J. & Jones, T. A. (1995). *Structure*, **3**, 535–540.

Kleywegt, G. J. & Jones, T. A. (1996). *Structure*, **4**, 1395–1400.

Kleywegt, G. J. & Jones, T. A. (1997). *Methods Enzymol.* **277**, 208–230.

Laskowski, R. A., MacArthur, M. W., Moss, D. S. & Thornton, J. M. (1993). *J. Appl. Cryst.* **26**, 283–291.

Lee, B. & Richards, F. M. (1971). *J. Mol. Biol.* **55**, 379–400.

Levin, M. S., Locke, B., Yang, N. C., Li, E. & Gordon, J. I. (1988). *J. Biol. Chem.* **263**, 17715–17723.

Li, E. & Norris, A. W. (1996). *Annu. Rev. Nutr.* **16**, 205–234.

Lotan, R. (1996). *FASEB J.* **10**, 1031–1039.

McPherson, A. J. (1982). *Preparation and Analysis of Protein Crystals.* New York: John Wiley.

Mangelsdorf, D. J., Thummel, C., Beato, M., Herrlich, P., Schütz, G., Umesono, K., Blumberg, B., Kastner, P., Mark, M., Chambon, P. & Evans, R. M. (1995). *Cell*, **83**, 835–839.

Morriss-Kay, G. M. & Sokolova, N. (1996). *FASEB J.* **10**, 961–968.

Napoli, J. L. (1996). *FASEB J.* **10**, 993–1001.

Navaza, J. (1994). *Acta Cryst.* A**50**, 157–163.

Newcomer, M. E. (1995). *FASEB J.* **9**, 229–239.

Ong, D. E. & MacDonald, P. N. (1987). *J. Biol. Chem.* **262**, 10550–10556.

Ong, D. E., Newcomer, M. E. & Chytil, F. (1994). *The Retinoids: Biology, Chemistry and Medicine*, edited by M. B. Sporn, A. B. Roberts & D. S. Goodman, pp. 283–317. New York: Raven Press.
Otwinowski, Z. & Minor, W. (1997). *Methods Enzymol.* **276**, 307–326.
Peck, G. L. & DiGiovanna, J. J. (1994). *The Retinoids: Biology, Chemistry and Medicine*, edited by M. B. Sporn, A. B. Roberts & D. S. Goodman, pp. 631–658. New York: Raven Press.
Ramakrishnan, C. & Ramachandran, G. N. (1965). *Biophys. J.* **5**, 909–933.
Read, R. J. (1986). *Acta Cryst.* A**42**, 140–149.
Ross, A. C. (1993). *FASEB J.* **7**, 317–327.
Rossmann, M. G. (1972). Editor. *The Molecular Replacement Method: A Collection of Papers on the Use of Non-Crystallographic Symmetry.* New York: Gordon & Breach.
Saari, J. C. (1994). *The Retinoids: Biology, Chemistry and Medicine*, edited by M. B. Sporn, A. B. Roberts & D. S. Goodman, pp. 351–385. New York: Raven Press.
Thompson, J. R., Bratt, J. M. & Banaszak, L. J. (1995). *J. Mol. Biol.* **252**, 433–446.
Tobita, T., Takeshita, A., Kitamura, K., Ohnishi, K., Yanagi, M., Hiraoka, A., Karasuno, T., Takeuchi, M., Miyawaki, S., Ueda, R., Naoe, T. & Ohno, R. (1997). *Blood*, **90**, 967–973.
Vriend, G. & Sander, C. (1993). *J. Appl. Cryst.* **26**, 47–60.